Radical−Molecule Reaction $C(^3P) + C_3H_6$: Mechanistic Study

Yan Li, Hui-ling Liu, Xu-ri Huang,* Yan-bo Sun, Zhuo Li, and Chia-chung Sun

State Key Laboratory of Theoretical and Computational Chemistry, Institute of Theoretical Chemistry, Jilin University, Changchun 130023, People's Republic of China

Received: April 27, 2009; Revised Manuscript Received: August 9, 2009

The complex triplet potential energy surface for the reaction of ground-state atomic carbon $C(^3P)$ with propylene C_3H_6 is explored at the B3LYP/6-311G(d,p), QCISD/6-311G(d,p), and G3B3 (single-point) levels. Various possible reaction pathways are probed. It is shown that the reaction is initiated by the addition of $C(^3P)$ to the C=C bond of C_3H_6 to generate barrierlessly the three-membered ring isomer **1** CH_3-cCHCCH$_2$, followed by the ring-opening process to form **2a** *trans*-CH_3CHCCH_2, which can easily interconvert to **2b** *cis*-CH_3CHCCH_2. Starting from **2** (**2a**, **2b**), the most feasible pathway is the internal C−H bond rupture of **2a** leading to $\mathbf{P_4}(^2CH_3CCCH_2 + {}^2H)$, terminal C−H bond cleavage of **2** (**2a**,**2b**) to form $\mathbf{P_5}(^2CH_3CHCCH + {}^2H)$, or direct C−C bond fission of **2b** to form $\mathbf{P_7}(^2CH_2CCH + {}^2CH_3)$, all of which may have comparable contributions to the title reaction. Much less competitively, **2a** takes a 1,2-H-shift to form **5a** *trans-cis*-$CH_3CHCHCH$, followed by a C−C bond rupture leading to $\mathbf{P_6}(^1C_2H_2 + {}^3CH_3CH)$. Because the intermediates and transition states involved in the feasible pathways all lie below the reactant, the title reaction is expected to be rapid, which is consistent with the measured large rate constant. The present article may provide some useful information for future experimental investigation of the title reaction.

1. Introduction

Carbon is believed to be the fourth most abundant element in universe and is ubiquitous in dense interstellar clouds (ISCs) where the temperature is very low. The reactions of ground-state atomic carbon $C(^3P)$ with unsaturated hydrocarbons are of great importance in interstellar chemistry,[1,2] hydrocarbon syntheses,[3,4] and combustion processes.[5−7] Accordingly, a large number of experimental and theoretical investigations have been reported on the atomic carbon $C(^3P)$ reactions with a variety of unsaturated hydrocarbons as well as their radicals such as acetylene (C_2H_2),[8−12] ethylene (C_2H_4),[13] propylene (C_3H_6),[14−17] *trans*-butylene (*trans*-C_4H_8),[17,18] allene (H_2CCCH_2),[17,19−21] propyne (CH_3CCH),[17,21,22] diacetylene (HCCCCH),[23] 1,3-butadiene ($H_2CCHCHCH_2$),[24] 1,2-butadiene ($H_2CCCHCH_3$),[25] propargyl (C_3H_3),[26] allyl (C_3H_5),[27] and so forth.

Among these studies, the reaction with propylene (C_3H_6) attracts our great interest. To our best knowledge, four experimental studies have already been performed on the $C(^3P) + C_3H_6$ reaction. In 1996, Kaiser et al.[14,15] investigated the title reaction using the crossed molecular beam technique. In these reports, the authors focused their attention on the methylpropargyl radical, C_4H_5 formation channel, which may represent an example of carbon−hydrogen exchange in the reactions of ground-state atomic carbon with unsaturated hydrocarbons. In 1999, Chastaing et al.[16] reported for the first time the rate constant of the $C(^3P) + C_3H_6$ reaction over the temperature range (15−295 K). The measured rate constant values indicate that the title reaction proceeds very rapidly and may play an important role in forming a long carbon chain in the ISM. In 2004, Loison et al.[17] studied the same reaction at room temperature in a low-pressure fast-flow reactor and obtained a rate constant of $k = (2.6 \pm 0.4) \times 10^{-10}$ cm^3 molecule^{-1} s^{-1}. In this article, three channels leading to H + CH_3CCCH_2, H + CH_3CHCCH, and CH_3 + C_3H_3 were proposed. In addition, they measured the absolute atomic hydrogen branching ratios of 0.51 ± 0.08 and suggested that H- and CH_3-elimination channels may compete with each other. However, without detailed potential energy surface investigations, it is difficult to discuss the mechanism of the $C(^3P) + C_3H_6$ reaction. Unfortunately, no theoretical study has been performed up to now. Therefore, in the present article, we carried out a detailed theoretical study on the title reaction to gain insight into the reaction mechanism and thereby to explain the experimental results.

2. Computational Methods

All calculations are performed using the Guassian 98 program package.[28] The geometries of all of the reactant, products, intermediates, and transition states are optimized using the B3LYP method in conjunction with the 6-311G(d,p) basis set. Frequency calculations are performed at the same level to check whether the obtained species is an isomer (with all real frequencies) or a transition state (with one and only one imaginary frequency). To obtain more reliable energetic data, single-point energy calculations are performed at the G3B3[29,30] level using the B3LYP/6-311G(d,p)-optimized geometries and scaled B3LYP/6-311G(d,p) zero-point energies. To confirm that the transition states connect designated intermediates, intrinsic reaction coordinate (IRC) calculations are carried out at the B3LYP/6-311G(d,p) level. Furthermore, for the most feasible channels, the structures are optimized at the QCISD/6-311G(d,p) level, followed by the G3B3 single-point energy calculations.

3. Results and Discussion

The optimized geometries of reactant and products are depicted in Figure 1, whereas the optimized geometries of

* Corresponding author.

10.1021/jp903844p CCC: $40.75
Published on Web 09/04/2009

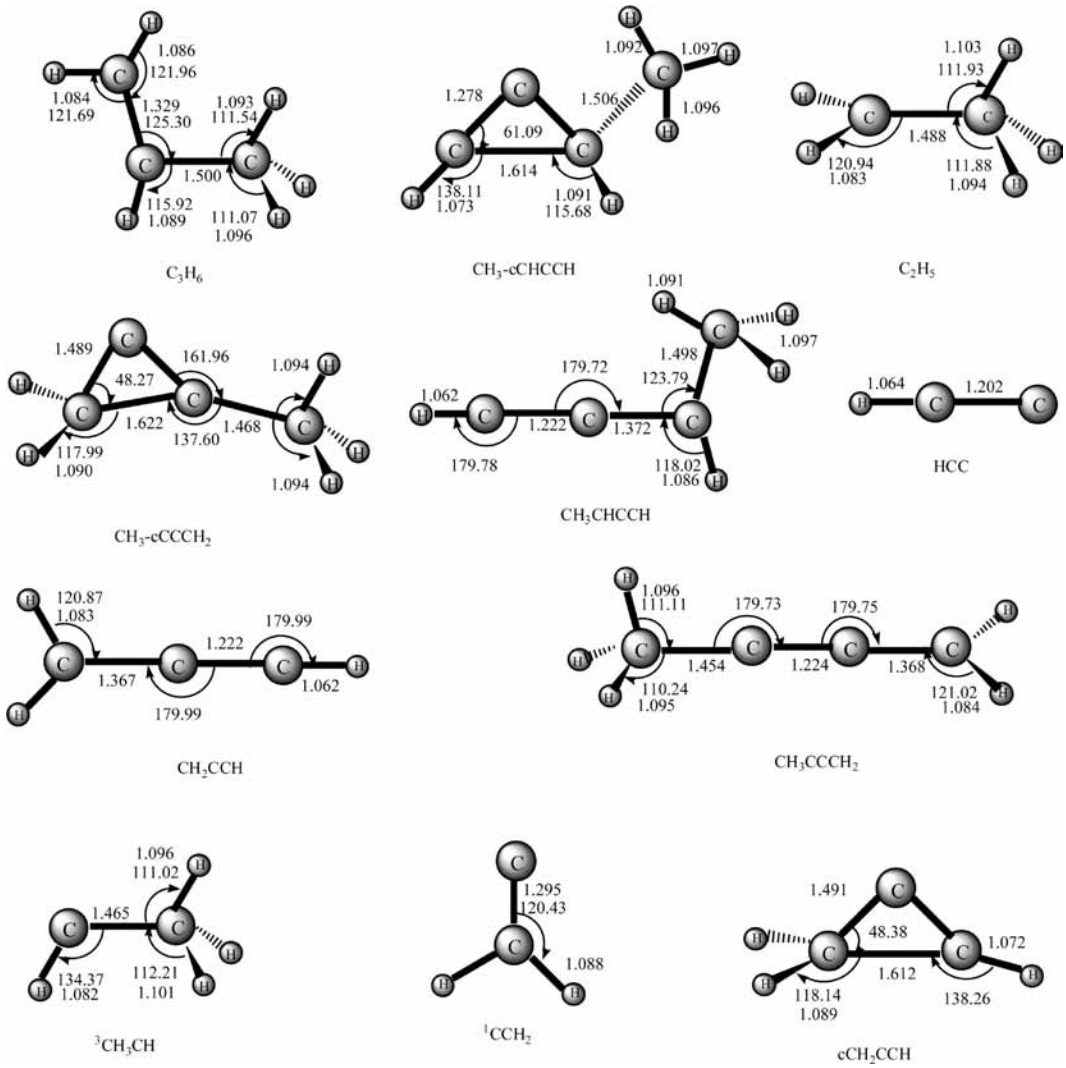

Figure 1. Optimized structures of the reactant and products. Distances are given in angstroms and angles are given in degrees.

intermediates and transitions are shown in Figures 2 and 3, respectively. The schematic potential energy surface (PES) of the C(^{3}P) + C_3H_6 reaction at the G3B3//B3LYP/6-311G(d,p) level is presented in Figure 4a,b. Table 1 lists the relative energies of reactant, products, intermediates, and transition states. Table 2 displays the vibrational frequencies (inverse centimeters) and moment of inertia (au) of the reactant, some important products, intermediates, and transition states. For convenient discussion, the energy of **R** (C(^{3}P) + C_3H_6) is set as zero for reference. The symbol **TSm/n** is used to denote the transition state connecting intermediates **m** and **n**. Unless otherwise specified, the G3B3//B3LYP/6-311G(d,p) energies are used throughout. Moreover, for the assessment of the G3B3//B3LYP/6-311G(d,p) results, the optimized QCISD/6-311G(d,p) geometries of the critical structures are shown in Figure 5, and the corresponding G3B3//QCISD/6-311G(d,p) energies are listed in Table 3.

3.1. Reaction Pathways. The ground-state atomic carbon C(^{3}P) attacks on the C=C double bond of C_3H_6 lead to the three-membered ring isomer **1** CH_3-cCHCCH$_2$. **1** is 52.0 kcal/mol more stable than the reactant **R** C(^{3}P) + C_3H_6, which means that the initial association provides **1** with enough energy to take subsequent changes. In the following parts, we will discuss the formation pathways of various products proceeding via **1**.

I. P_1(^{2}CH$_3$-cCHCCH + ^{2}H) and P_2(^{2}CH$_3$cCCCH$_2$ + ^{2}H). **1** CH_3-cCHCCH$_2$ (−52.0) can undergo H-elimination to lead to two different weakly bound complexes **10** CH_3-cCHCCH···H (−6.6) and **11** CH_3-cC(···H)CCH$_2$ (−9.4). Subsequently, **10** and **11** can dissociate to $\mathbf{P_1}$ ^{2}CH$_3$-cCHCCH + ^{2}H (−7.0) and $\mathbf{P_2}$ ^{2}CH$_3$-cCCCH$_2$ + ^{2}H (−9.6), respectively. The values in parentheses are G3B3//B3LYP/6-311G(d,p) relative energies in kilocalories per mole with respect to reactant **R** C(^{3}P) + C_3H_6 (0.0). The formation pathways of $\mathbf{P_1}$ and $\mathbf{P_2}$ can be written as

Path P_1

$$\mathbf{R \rightarrow 1 \rightarrow 10 \rightarrow P_1}$$

Path P_2

$$\mathbf{R \rightarrow 1 \rightarrow 11 \rightarrow P_2}$$

II. P_3(c^{2}CH$_2$CCH + ^{2}CH$_3$). **1** CH_3-cCHCCH$_2$ (−52.0) undergoes CH_3 elimination to lead to $\mathbf{P_3}$ c^{2}CH$_2$CCH + ^{2}CH$_3$ (−14.9). Such a simple process can be written as

Path P_3

$$\mathbf{R \rightarrow 1 \rightarrow P_3}$$

III. $P_4(^2CH_3CCCH_2 + {}^2H)$. From Figure 4a, we find that five pathways are possible to form $\mathbf{P_4}$ $^2CH_3CCCH_2 + {}^2H$ (−50.1). They can be written as

Path $P_4(1)$

$$\mathbf{R \rightarrow 1 \rightarrow 2a \rightarrow 3 \rightarrow P_4}$$

Path $P_4(2)$

$$\mathbf{R \rightarrow 1 \rightarrow 2a \rightarrow 4 \rightarrow 6 \rightarrow P_4}$$

Path $P_4(3)$

$$\mathbf{R \rightarrow 1 \rightarrow 2a \rightarrow 5a \rightarrow 5b \rightarrow 6 \rightarrow P_4}$$

Path $P_4(4)$

$$\mathbf{R \rightarrow 1 \rightarrow 2a \rightarrow 5b \rightarrow 6 \rightarrow P_4}$$

Path $P_4(5)$

$$\mathbf{R \rightarrow 1 \rightarrow 2a \rightarrow 6 \rightarrow P_4}$$

1 CH_3-cCHCCH$_2$ (−52.0) can transform to **2a** *trans*-CH_3CHCCH_2 (−83.8) via a ring-opening process. Subsequently, **2a** undergoes H-elimination to form the weakly bound complex

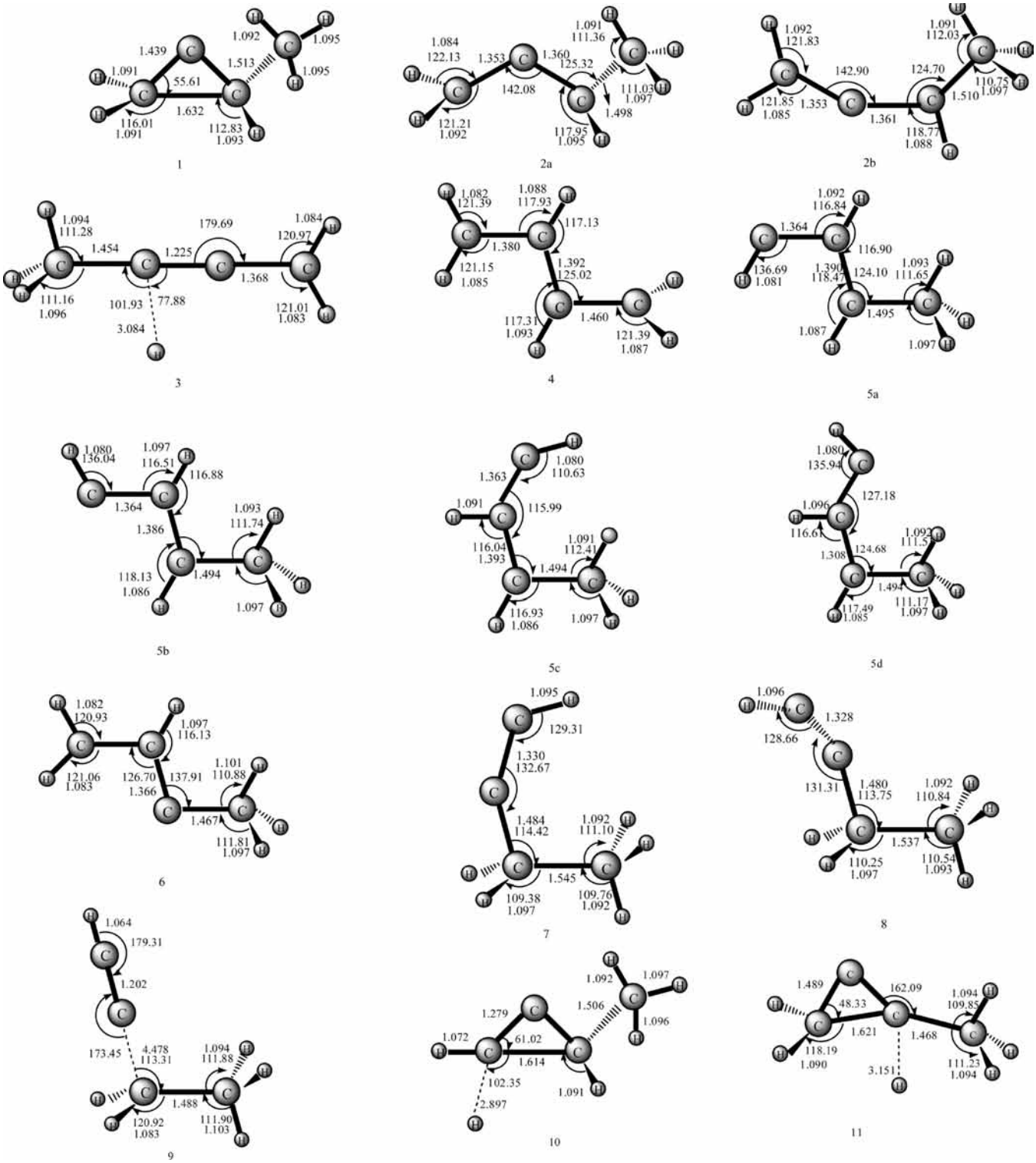

Figure 2. Optimized structures of the intermediates. Distances are given in angstroms and angles are given in degrees.

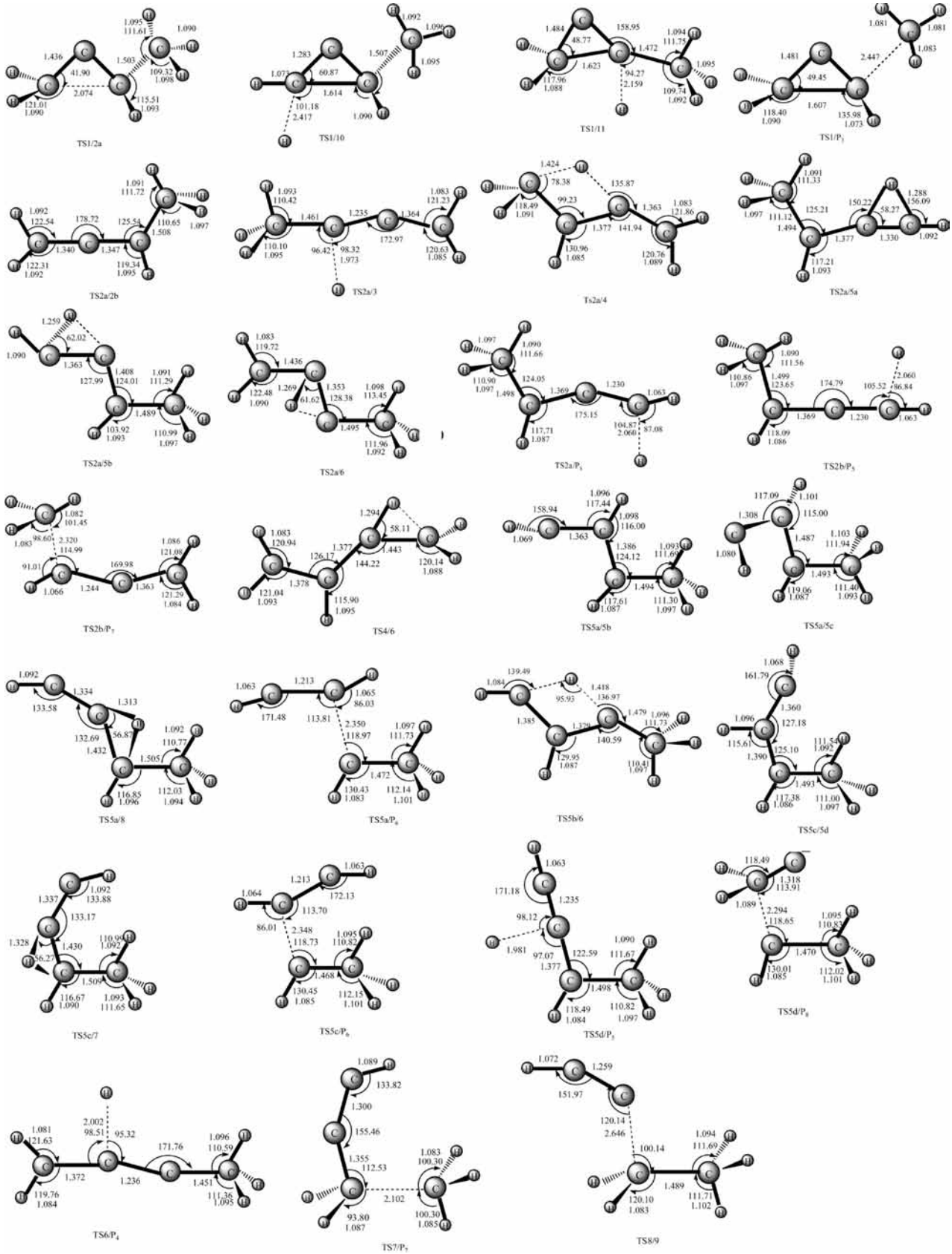

Figure 3. Optimized structures of the transition states. Distances are given in angstroms and angles are given in degrees.

3 $CH_3C(\cdots H)CCH_2$ (−49.8) before the final product **P**$_4$($^2CH_3CCCH_2 + {}^2H$) (−50.1), as in **Path P$_4$(1)**. Alternatively, **P**$_4$ can be produced via **6** CH_3CCHCH_2 (−85.4) through H-elimination. Intermediate **6** can be formed through four channels, that is, (i) successive 1,3- and 1,2-H-shift of **2a** to form **4** $CH_2CHCHCH_2$ (−89.8) and **6**, as in **Path P$_4$(2)**, (ii) successive 1,2-H-shift, *cis-trans* isomerization, and 1,3-H-shift to produce **5a** *trans-cis*-$CH_3CHCHCH$ (−82.3), **5b** *trans-trans*-

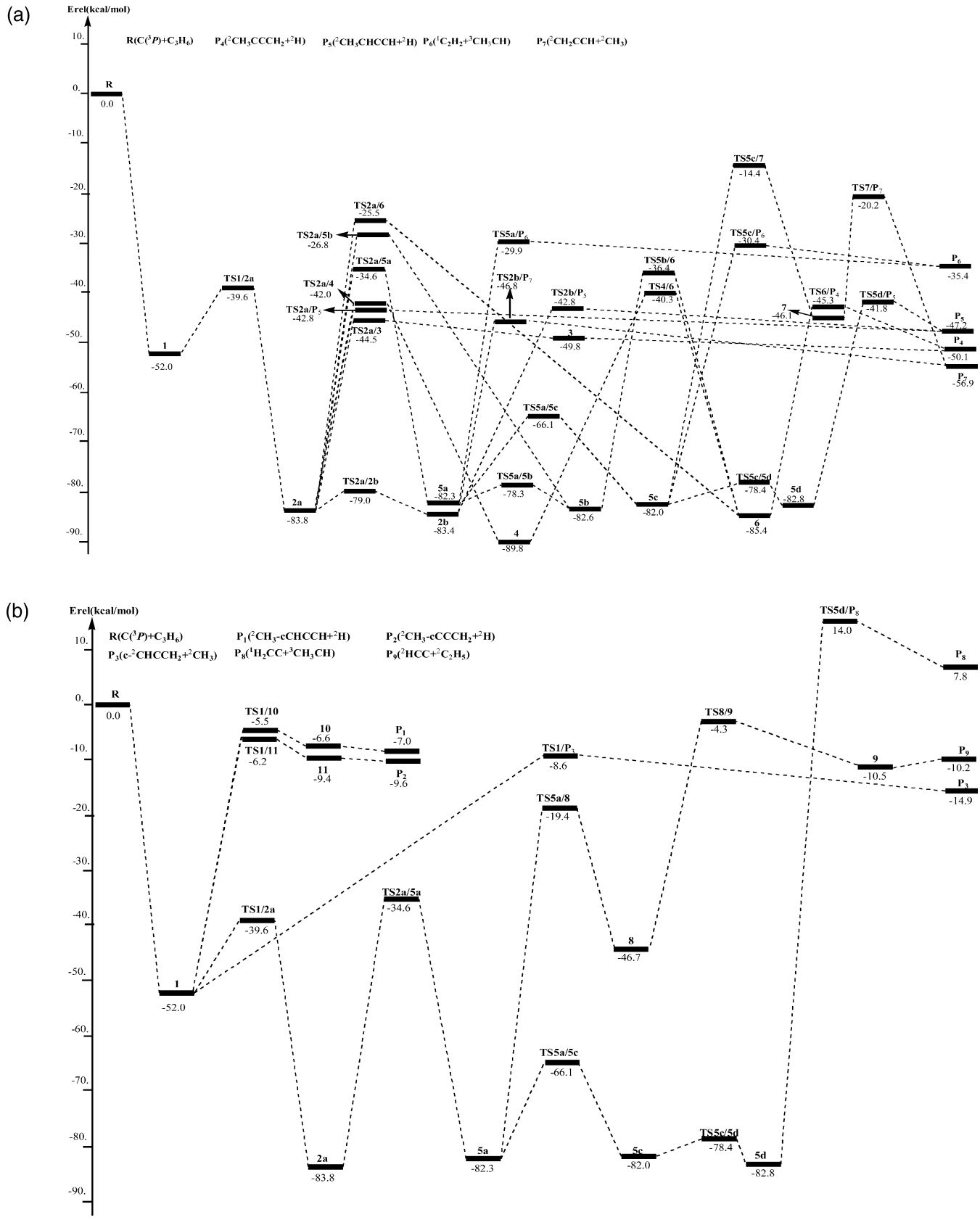

Figure 4. (a) Schematic potential energy surface (PES) of the most favorable products P_4($^2CH_3CCCH_2$ + ^2H), P_5($^2CH_3CHCCH$ + ^2H), P_6($^1C_2H_2$ + $^3CH_3CH$), and P_7($^2CH_2CCH$ + $^2CH_3$) for the C(^{3}P) + C_3H_6 reaction. (b) Schematic PES of the unfavorable products P_1($^2CH_3$-cCHCCH + ^2H), P_2($^2CH_3$-cCCCH$_2$ + ^2H), P_3(c$^2CH_2CCH$ + $^2CH_3$), P_8($^1CCH_2$ + $^3CH_3CH$), and P_9(^2HCC + $^2C_2H_5$) for the C(^{3}P) + C_3H_6 reaction.

$CH_3CHCHCH$ (−82.6), and **6**, as in **Path P_4(3)**, (iii) continuous 1,2- and 1,3-H-shift of **2a** to form **5b** and **6** as in **Path P_4(4)**, (iv) 2,3-H-shift of **2a** to form **6** as in **Path P_4(4)**.

For **2** → **P_4** conversion, only one barrier 39.3 (**2a** → **3**) kcal/mol needs to climbed in **Path P_4(1)**, whereas more barriers have to be surmounted in the latter four pathways,

that is, 41.8 (**2a** → **4**), 49.5 (**4** → **6**), and 40.1 (**6** → $\mathbf{P_4}$) kcal/mol in **Path P_4(2)**, 49.2 (**2a** → **5a**), 46.2 (**5b** → **6**), and 40.1 (**6** → $\mathbf{P_4}$) kcal/mol in **Path P_4(3)**, 57.0 (**2a** → **5b**), 46.2 (**5b** → **6**), and 40.1 (**6** → $\mathbf{P_4}$) kcal/mol in **Path P_4(4)**, and 58.3 (**2a** → **6**) and 40.1 (**6** → $\mathbf{P_4}$) kcal/mol in **Path P_4(5)**. Obviously, the optimal channel to form $\mathbf{P_4}$ is **Path P_4(1)**.

IV. P_5($^2CH_3CHCCH + {}^2H$). For product $\mathbf{P_5}$ $^2CH_3CHCCH + {}^2H$ (−47.2), there are three possible energetic pathways

Path P_5(1)

$$\mathbf{R \rightarrow 1 \rightarrow 2a \rightarrow P_5}$$

Path P_5(2)

$$\mathbf{R \rightarrow 1 \rightarrow 2a \rightarrow 2b \rightarrow P_5}$$

Path P_5(3)

$$\mathbf{R \rightarrow 1 \rightarrow 2a \rightarrow 5a \rightarrow 5c \rightarrow 5d \rightarrow P_5}$$

2a *trans*-CH_3CHCCH_2 (−83.8) can easily interconvert to **2b** *cis*-CH_3CHCCH_2 (−83.4); then, both **2a** and **2b** can lead to $\mathbf{P_5}$ via C−H bond rupture, as in **Path P_5(1)** and **Path P_5(2)**. The formation of **5a** *trans-cis*-$CH_3CHCHCH$ (−82.3) is the same as that in **Path P_4(3)**. **5a** can continuously isomerize to **5c** *cis-cis*-$CH_3CHCHCH$ (−82.0) and then to **5d** *cis-trans*-$CH_3CHCHCH$ (−85.4), followed by H-elimination to generate $\mathbf{P_5}$, as in **Path P_5(3)**.

In **Path P_5(3)**, two high barriers need to be surmounted from **2a** to $\mathbf{P_5}$, that is, 49.2 and 41.0 kcal/mol for **2a** → **5a** and **5d** → $\mathbf{P_5}$ conversions, respectively, yet only one barrier 41.0 (**2a** → $\mathbf{P_5}$) kcal/mol in **Path P_5(1)** and 40.6 (**2b**→$\mathbf{P_5}$) kcal/mol in **Path P_5(2)** is needed. Therefore, **Path P_5(3)** should be less competitive than **Path P_5(1)** and **Path P_5(2)**, which may compete with each other.

V. P_6($^1C_2H_2 + {}^3CH_3CH$). For product $\mathbf{P_6}$ $^1C_2H_2 + {}^3CH_3CH$ (−35.4), two pathways are energetically possible.

Path P_6(1)

$$\mathbf{R \rightarrow 1 \rightarrow 2a \rightarrow 5a \rightarrow P_6}$$

Path P_6(2)

$$\mathbf{R \rightarrow 1 \rightarrow 2a \rightarrow 5a \rightarrow 5c \rightarrow P_6}$$

The formation of **5a** *trans-cis*-$CH_3CHCHCH$ (−82.3) is the same as that in **Path P_4(3)**. Subsequently, **5a** can undergo either direct C−C bond rupture to form $\mathbf{P_6}$, as in path **P_6(1)**, or *cis-trans* isomerization to give **5c** *cis-cis*-$CH_3CHCHCH$ (−82.0), followed by dissociation to form $\mathbf{P_6}$, as in **Path P_6(2)**.

For **5a** → $\mathbf{P_6}$ conversion, two barriers need to be climbed in **Path P_6(2)**, that is, 16.2 and 51.6 kcal/mol for the steps of **5a** → **5c** and **5c** → $\mathbf{P_6}$, respectively, yet only one barrier 52.4 (**5a** → $\mathbf{P_6}$) kcal/mol is needed to surmount in **Path P_6(1)**. Then, we expect that path **P_6(1)** should be the optimal channel to form $\mathbf{P_6}$.

VI. P_7($^2CH_2CCH + {}^2CH_3$). There are two feasible pathways to produce $\mathbf{P_7}$ $^2CH_2CCH + {}^2CH_3$ (−56.9), which can be depicted as

Path P_7(1)

$$\mathbf{R \rightarrow 1 \rightarrow 2a \rightarrow 2b \rightarrow P_7}$$

Path P_7(2) $\mathbf{R \rightarrow 1 \rightarrow 2a \rightarrow 5a \rightarrow 5c \rightarrow 7 \rightarrow P_7}$

The formation of **2b** *cis*-CH_3CHCCH_2 (−83.4) is the same as that in **Path P_5(2)**. Subsequently, **2b** undergoes C−C bond cleavage to yield $\mathbf{P_7}$, as in **Path P_7(1)**. The barrier for **2b** → $\mathbf{P_7}$ conversion is 36.6 kcal/mol. In path **P_7(2)**, the formation of **5c** *cis-cis*-$CH_3CHCHCH$(−82.0) is the same as that in **Path P_5(2)**. Then, **5c** undergoes a 2,3-H-shift to form **7** *p*-CH_3CH_2CCH (−46.1), followed by C−C bond cleavage to lead to $\mathbf{P_7}$. The high barrier 67.6 (**5c** → **7**) kcal/mol involved in **Path P_7(2)** makes it less competitive than **Path P_7(1)**.

TABLE 1: Total (au) and Relative Energies in Parentheses (kilocalories per mole) of the Reactant, Products, Intermediates, and Transition States for the B3LYP/6-311G(d,p) and G3B3//B3LYP/6-311G(d,p) Levels

species	B3LYP	G3B3		species	B3LYP	G3B3	
R($C(^3P) + C_3H_6$)	−155.8000368	−155.6178692	(0.0)	**TS1/2a**	−155.8701580	−155.6809243	(−39.6)
P_1($^2CH_3$-cCHCCH + ^2H)	−155.8024541	−155.6290539	(−7.0)	**TS1/10**	−155.8025851	−155.6266115	(−5.5)
P_2($^2CH_3$-cCCCH$_2$ + ^2H)	−155.8078289	−155.6331102	(−9.6)	**TS1/11**	−155.8068104	−155.6277462	(−6.2)
P_3($c^2CH_2CCH + {}^2CH_3$)	−155.8228438	−155.6415604	(−14.9)	**TS1/P_3**	−155.8175318	−155.6316477	(−8.6)
P_4($^2CH_3CCCH_2 + {}^2H$)	−155.8752393	−155.6976681	(−50.1)	**TS2a/2b**	−155.9378914	−155.7437994	(−79.0)
P_5($^2CH_3CHCCH + {}^2H$)	−155.8694903	−155.6931650	(−47.2)	**TS2a/3**	−155.8725119	−155.6888489	(−44.5)
P_6($^1C_2H_2 + {}^3CH_3CH$)	−155.8552952	−155.6742567	(−35.4)	**TS2a/4**	−155.8730956	−155.6847667	(−42.0)
P_7($^2CH_2CCH + {}^2CH_3$)	−155.8911135	−155.7084670	(−56.9)	**TS2a/5a**	−155.8602317	−155.6730691	(−34.6)
P_8($^1CCH_2 + {}^3CH_3CH$)	−155.7858926	−155.6055080	(7.8)	**TS2a/5b**	−155.8499603	−155.6606230	(−26.8)
P_9($^2HCC + {}^2C_2H_5$)	−155.8131105	−155.6341069	(−10.2)	**TS2a/6**	−155.8476532	−155.6585450	(−25.5)
1	−155.8906157	−155.7007989	(−52.0)	**TS2a/P_5**	−155.8679075	−155.6860213	(−42.8)
2a	−155.9445822	−155.7513619	(−83.8)	**TS2b/P_5**	−155.8678899	−155.6861128	(−42.8)
2b	−155.9435455	−155.7507397	(−83.4)	**TS2b/P_7**	−155.8802263	−155.6924323	(−46.8)
3	−155.8754285	−155.6972995	(−49.8)	**TS4/6**	−155.8710656	−155.6820832	(−40.3)
4	−155.9516311	−155.7609420	(−89.8)	**TS5a/5b**	−155.9325716	−155.7426641	(−78.3)
5a	−155.9400304	−155.7489751	(−82.3)	**TS5a/5c**	−155.9113882	−155.7231904	(−66.1)
5b	−155.9407140	−155.7495029	(−82.6)	**TS5a/8**	−155.8286435	−155.6487535	(−19.4)
5c	−155.9392554	−155.7485115	(−82.0)	**TS5a/P_6**	−155.8480027	−155.6655362	(−29.9)
5d	−155.9408877	−155.7497830	(−82.8)	**TS5b/6**	−155.8631758	−155.6759254	(−36.4)
6	−155.9468650	−155.7538995	(−85.4)	**TS5c/5d**	−155.9326797	−155.7428369	(−78.4)
7	−155.8787106	−155.6913884	(−46.1)	**TS5c/7**	−155.8294587	−155.6407892	(−14.4)
8	−155.8800735	−155.6923504	(−46.7)	**TS5c/P_6**	−155.8487022	−155.6663904	(−30.4)
9	−155.8132832	−155.6345247	(−10.5)	**TS5d/P_5**	155.8658829	−155.6844717	(−41.8)
10	−155.8026574	−155.6283747	(−6.6)	**TS5d/P_8**	−155.7801320	−155.5955092	(14.0)
11	−155.8079694	−155.6328777	(−9.4)	**TS6/P_4**	−155.8730725	−155.6900799	(−45.3)
				TS7/P_7	−155.8378281	−155.6499807	(−20.2)
				TS8/9	−155.8091742	−155.6247063	(−4.3)

TABLE 2: Vibrational Frequencies and Moment of Inertia of Reactant, Some Important Products, Intermediates, and Transition States at the B3LYP/6-311G(d,p) Level of Theory

species	moment of inertia (au)			frequencies (cm^{-1})
C_3H_6	38.4	194.5	221.8	205, 425, 591, 924, 942, 948, 1030, 1071, 1189, 1327, 1408, 1449, 1481, 1495, 1713, 3013, 3056, 3092, 3120, 3127, 3208
CH_3CCCH_2	17.5	499.8	506.1	23, 179, 206, 383, 412, 667, 772, 1030, 1031, 1052, 1261, 1414, 1465, 1473, 1474, 2148, 3006, 3055, 3072, 3132, 3219
CH_3CHCCH	46.4	407.9	443.1	92, 211, 381, 435, 552, 598, 645, 868, 1007, 1098, 1152, 1390, 1404, 1477, 1494, 2015, 2997, 3032, 3111, 3148, 3469
CH_3CH	13.0	73.5	75.2	191, 761, 994, 1071, 1101, 1388, 1454, 1454, 2943, 2978, 3045, 3206
C_2H_2	0.0	50.6	50.6	642, 642, 773, 773, 2070, 3421, 3524
CH_2CCH	6.2	188.5	194.7	352, 403, 469, 638, 682, 1031, 1089, 1456, 2011, 3139, 3230, 3468
CH_3	6.3	6.3	12.6	505, 1403, 1403, 3104, 3283, 3283
1	93.6	278.7	307.8	211, 333, 387, 639, 844, 879, 900, 994, 1029, 1064, 1091, 1117, 1245, 1372, 1404, 1470, 1485, 1494, 3019, 2043, 3048, 3074, 3103, 3110
2a	38.4	462.1	489.4	128, 215, 255, 461, 565, 742, 781, 858, 962, 1020, 1113, 1175, 1308, 1400, 1439, 1469, 1477, 1509, 2999, 3032, 3036, 3056, 3111, 3178
2b	79.5	362.9	431.3	99, 191, 399, 490, 516, 746, 776, 869, 994, 1012, 1072, 1126, 1347, 1388, 1437, 1467, 1475, 1501, 3003, 3044, 3054, 3104, 3124, 3172
3	49.6	499.8	538.2	20, 34, 62, 101, 179, 207, 207, 380, 412, 668, 773, 1029, 1029, 1054, 1262, 1414, 1464, 1472, 1474, 2144, 3009, 3057, 3075, 3134, 3221
5a	45.0	426.6	460.5	148, 218, 287, 483, 582, 746, 842, 921, 927, 1026, 1119, 1215, 1243, 1349, 1410, 1459, 1474, 1505, 2997, 3031, 3081, 3090, 3144, 3222
TS1/2a	75.5	357.6	374.1	493i, 87, 300, 405, 545, 641, 764, 893, 939, 1015, 1080, 1118, 1229, 1365, 1388, 1441, 1477, 1488, 3006, 3057, 3062, 3072, 3122, 3163
TS2a/2b	52.2	443.7	484.8	256i, 107, 348, 379, 507, 759, 816, 835, 954, 1013, 1055, 1108, 1338, 1390, 1452, 1476, 1484, 1587, 2998, 3015, 3031, 3040, 3075, 3113
TS2a/3	34.1	498.7	521.7	596i, 119, 200, 202, 347, 420, 425, 502, 668, 776, 1016, 1037, 1047, 1258, 1411, 1454, 1469, 1476, 2064, 3018, 3072, 3088, 3128, 3217
TS2a/5a	40.6	453.2	482.7	2133i, 109, 160, 237, 319, 502, 624, 761, 834, 874, 1015, 1097, 1157, 1357, 1405, 1475, 1488, 1598, 2280, 2998, 3033, 3038, 3062, 3107
TS2a/P_5	52.6	444.9	486.3	521i, 90, 181, 186, 320, 400, 445, 565, 624, 750, 866, 1008, 1094, 1150, 1384, 1405, 1476, 1494, 1964, 3001, 3038, 3113, 3140, 3455
TS2b/P_5	67.3	412.7	468.8	517i, 89, 172, 213, 336, 394, 440, 564, 625, 749, 870, 1006, 1095, 1146, 1382, 1401, 1476, 1493, 1962, 3001, 3039, 3117, 3145, 3454
TS2b/P_7	95.9	489.1	572.6	475i, 21, 121, 327, 346, 406, 484, 495, 525, 690, 710, 825, 1011, 1082, 1413, 1420, 1452, 1864, 3089, 3115, 3200, 3247, 3256, 3400
TS5a/P_6	62.9	589.3	640.9	347i, 37, 73, 140, 240, 269, 578, 634, 755, 771, 808, 992, 1077, 1102, 1392, 1456, 1462, 1952, 2946, 2979, 3034, 3199, 3397, 3487

VII. $P_8(^1CCH_2 + {}^3CH_3CH)$, $P_9(^2HCC + {}^2C_2H_5)$. Only one feasible pathway is associated with the formation of $\mathbf{P_8}$ $^1CCH_2 + {}^3CH_3CH$ (7.8) and $\mathbf{P_9}$ $^2HCC + {}^2C_2H_5$ (−10.2), which can be written as

Path P_8

$$\mathbf{R \rightarrow 1 \rightarrow 2a \rightarrow 5a \rightarrow 5c \rightarrow 5d \rightarrow P_8}$$

Path P_9

$$\mathbf{R \rightarrow 1 \rightarrow 2 \rightarrow 5a \rightarrow 8 \rightarrow 9 \rightarrow P_9}$$

Path P_8 is very similar to **Path P_5(3)**. The difference lies in the last dissociation step; that is, in **Path P_5(3)**, **5d** *cis-trans*-$CH_3CHCHCH$ (−82.8) leads to $\mathbf{P_5}$ $^2CH_3CHCCH + {}^2H$ (−47.2) via the C−H bond rupture, whereas in **Path P_8**, **5d** gives rise to $\mathbf{P_8}$ via the concerted 1,2-H-shift and C−C bond rupture. The barrier for the step of **7d** → $\mathbf{P_8}$ is 96.8 kcal/mol.

In **Path P_9**, **5a** *trans-cis*-$CH_3CHCHCH$ (−82.3) undergoes a 2,3-H-shift to give **8** *v*-CH_3CH_2CCH (−46.7) with the barrier of 62.9 kcal/mol. Subsequently, **8** can undergo internal C−C bond rupture to form the weakly bound complex **9** $C_2H_5\cdots CCH$ (−10.5) before the final product $\mathbf{P_9}$. The barrier for the step of **8** → **9** is 42.4 kcal/mol.

4. Reaction Mechanism

In the preceding sections, we have obtained nine products, that is $\mathbf{P_1}$($^2CH_3$-cCHCCH + ^2H), $\mathbf{P_2}$($^2CH_3$-cCCCH$_2$ + ^2H), $\mathbf{P_3}$(c$^2CH_2CCH$ + $^2CH_3$), $\mathbf{P_4}$($^2CH_3CCCH_2$ + ^2H), $\mathbf{P_5}$($^2CH_3$CHCCH + ^2H), $\mathbf{P_6}$($^1C_2H_2$ + $^3CH_3CH$), $\mathbf{P_7}$($^2CH_2CCH$ + $^2CH_3$), $\mathbf{P_8}$($^1CCH_2$ + $^3CH_3CH$), and $\mathbf{P_9}$(^2HCC + $^2C_2H_5$). For easier

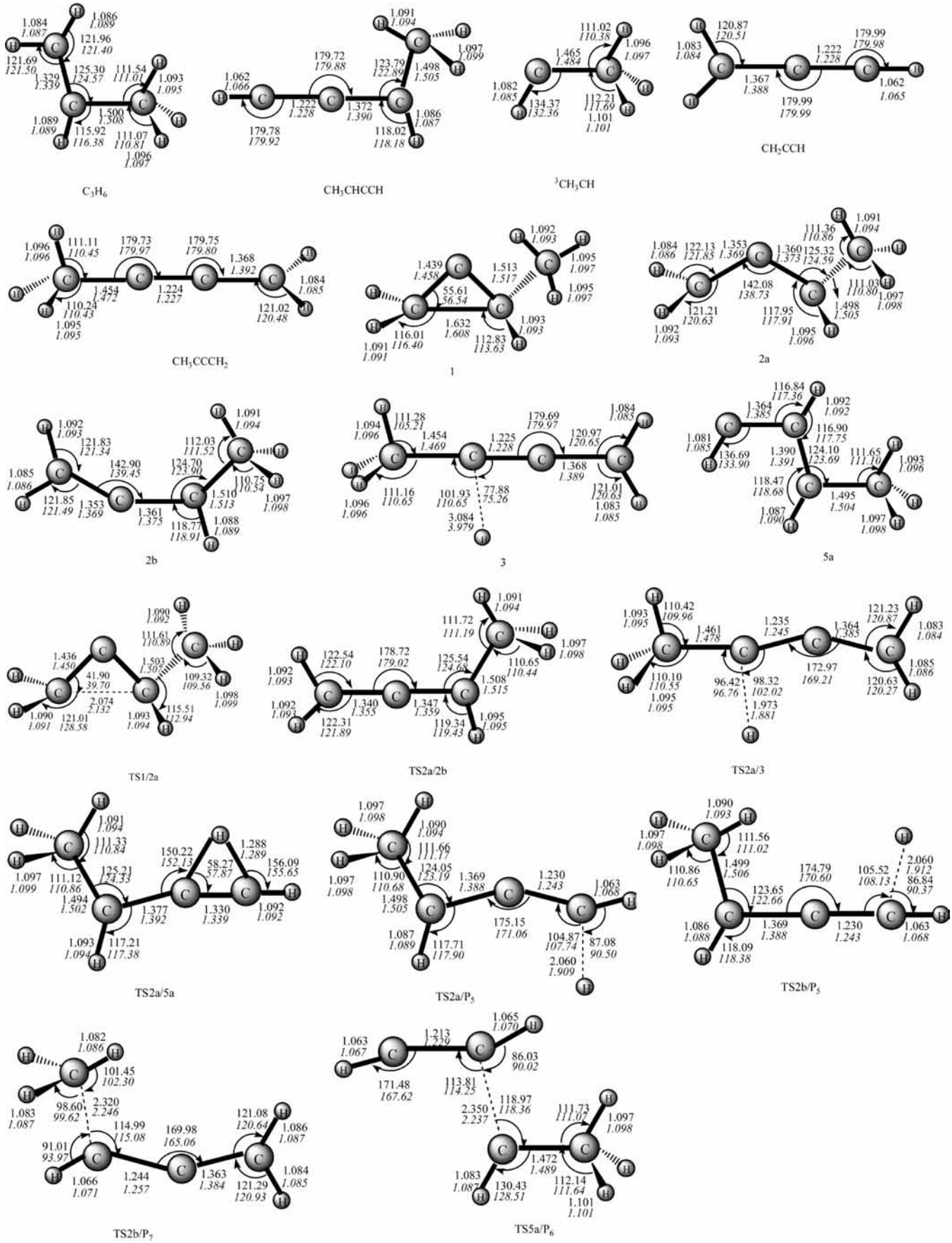

Figure 5. Optimized structures of the species involved in the most feasible channels at B3LYP/6-311G(d,p) and QCISD/6-311G(d,p) (in italic) levels.

TABLE 3: Total (au) and Relative Energies in Parentheses (kilocalories per mole) of the Critical Structures for the $C(^3P) + C_3H_6$ Reaction

species	G3B3//B3LYP/6-311G(d,p)		G3B3//QCISD/6-311G(d,p)	
$R(C(^3P) + C_3H_6)$	−155.6178692	(0.0)	−155.6171371	(0.0)
$P_4(^2CH_3CCH_2 + {}^2H)$	−155.6976681	(−50.1)	−155.6971700	(−50.2)
$P_5(^2CH_3CHCCH + {}^2H)$	−155.6931650	(−47.2)	−155.6928531	(−47.5)
$P_6(^1C_2H_2 + {}^3CH_3CH)$	−155.6742567	(−35.4)	−155.6736507	(−35.5)
$P_7(^2CH_2CCH + {}^2CH_3)$	−155.7084670	(−56.9)	−155.7083056	(−57.2)
1	−155.7007989	(−52.0)	−155.6990873	(−51.4)
2a	−155.7513619	(−83.8)	−155.7505645	(−83.7)
2b	−155.7507397	(−83.4)	−155.7500858	(−83.4)
3	−155.6972995	(−49.8)	−155.6972234	(−50.3)
5a	−155.7489751	(−82.3)	−155.7480220	(−82.1)
TS1/2a	−155.6809243	(−39.6)	−155.6787693	(−38.7)
TS2a/2b	−155.7437994	(−79.0)	−155.7430849	(−79.0)
TS2a/3	−155.6888489	(−44.5)	−155.6879900	(−44.5)
TS2a/5a	−155.6730691	(−34.6)	−155.6724964	(−34.7)
TS2a/P_5	−155.6860213	(−42.8)	−155.6847208	(−42.4)
TS2b/P_5	−155.6861128	(−42.8)	−155.6849160	(−42.5)
TS2b/P_7	−155.6924323	(−46.8)	−155.6919340	(−46.9)
TS5a/P_6	−155.6655362	(−29.9)	−155.6640196	(−29.4)

discussion, the most feasible formation pathways of these nine products are listed again

Path P_1

$$\mathbf{R \rightarrow 1 \rightarrow 10 \rightarrow P_1}$$

Path P_2

$$\mathbf{R \rightarrow 1 \rightarrow 11 \rightarrow P_2}$$

Path P_3

$$\mathbf{R \rightarrow 1 \rightarrow P_3}$$

Path P_4(1)

$$\mathbf{R \rightarrow 1 \rightarrow 2a \rightarrow 3 \rightarrow P_4}$$

Path P_5(1)

$$\mathbf{R \rightarrow 1 \rightarrow 2a \rightarrow P_5}$$

Path P_5(2)

$$\mathbf{R \rightarrow 1 \rightarrow 2a \rightarrow 2b \rightarrow P_5}$$

Path P_6(1)

$$\mathbf{R \rightarrow 1 \rightarrow 2a \rightarrow 5a \rightarrow P_6}$$

Path P_7(1)

$$\mathbf{R \rightarrow 1 \rightarrow 2a \rightarrow 2b \rightarrow P_7}$$

Path P_8

$$\mathbf{R \rightarrow 1 \rightarrow 2a \rightarrow 5a \rightarrow 5c \rightarrow 5d \rightarrow P_8}$$

Path P_9

$$\mathbf{R \rightarrow 1 \rightarrow 2a \rightarrow 5a \rightarrow 8 \rightarrow 9 \rightarrow P_9}$$

Product $\mathbf{P_8}$ (7.8) with positive relative energies is surely thermodynamically not accessible. Products $\mathbf{P_1}$ (−7.0), $\mathbf{P_2}$ (−9.6), $\mathbf{P_3}$ (−14.9), and $\mathbf{P_9}$ (−10.2) lie rather high; this thermodynamically prevents their experimental observation with detected yields relative to $\mathbf{P_4}$ (−50.1), $\mathbf{P_5}$ (−47.2), $\mathbf{P_6}$ (−35.4), and $\mathbf{P_7}$ (−56.9). As for products $\mathbf{P_4}$, $\mathbf{P_5}$, $\mathbf{P_6}$, and $\mathbf{P_7}$, $\mathbf{P_6}$ should be the least feasible product because of the high barriers 49.2 (**2a** → **5a**) and 52.4 (**5a** → $\mathbf{P_6}$) kcal/mol involved in **Path P_6(1)**. It seems very difficult to compare the feasibility of **Path P_4(1)**, **Path P_5(1)**, **Path P_5(2)**, and **Path P_7(1)** because the barriers 39.3 (**2a** → **3**) kcal/mol in **Path P_4(1)**, 41.0 (**2a** → $\mathbf{P_5}$) kcal/mol in **Path P_5(1)**, 40.6 (**2b** → $\mathbf{P_5}$) kcal/mol in **Path P_5(2)**, and 36.6 (**2b** → $\mathbf{P_7}$) kcal/mol in **Path P_7(1)** are very close. Then, we tentatively expect that these four pathways may have comparable contribution to the title reaction.

As a result, reflected in the final products, a total of four kinds of products may be observed. $\mathbf{P_4}$, $\mathbf{P_5}$, and $\mathbf{P_7}$ are the most favorable products, $\mathbf{P_6}$ is the much less competitive product. The branching ratios of $\mathbf{P_5}$ may be twice as much as that of $\mathbf{P_4}$ and $\mathbf{P_7}$.

5. Comparison with Experiments

There have been four experimental studies concerning the $C(^3P) + C_3H_6$ reaction. The studies by Kaiser et al.[14,15] indicate that the title reaction is initiated by the addition of carbon atom to the C═C bond of C_3H_6 to form methylcyclopropylidene, followed by ring-opening to 1,2-butadiene. Subsequently, 1,2-butadiene can undergo H-elimination lead to $C_4H_5 + H$. Methylcyclopropylidene, 1,2-butadiene, and $C_4H_5 + H$ correspond to **1** CH_3-c$CHCCH_2$, **2a** *trans*-CH_3CHCCH_2, and $\mathbf{P_4}(^2CH_3CCCH_2 + {}^2H)$ or $\mathbf{P_5}(^2CH_3CHCCH + {}^2H)$, respectively, in our theoretical studies. Obviously, the experimental findings obtained by Kaiser et al. are in excellent agreement with our calculation results. In addition, the overall barrierless association, isomerization, and dissociation processes of the title reaction can account for the large rate constant obtained by Chastaing et al.[16] Furthermore, Loison et al.[17] studied the same reaction at room temperature, and three channels leading to products $H + CH_3CCCH_2$, $H + CH_3CHCCH$, and $CH_3 + C_3H_3$ are proposed. Moreover, on the basis of the absolute atomic hydrogen branching ratios of 0.51 ± 0.08, Loison et al. suggested that H- and CH_3-elimination channels may compete with each other. Products $H + CH_3CCCH_2$, $H + CH_3CHCCH$, and $CH_3 + C_3H_3$ correspond to $\mathbf{P_4}$, $\mathbf{P_5}$, and $\mathbf{P_7}$, respectively. In this aspect, the results by Loison et al. agree well with our theoretical calculations. However, on the basis of our results, **Path P_4(1)**, **Path P_5(1)**, **Path P_5(2)**, and **Path P_7(1)** may have comparable contribution to the $C(^3P) + C_3H_6$ reaction. In other words, among the final product distributions, the atomic hydrogen should have a larger branching ratio than that of $CH_3 + C_3H_3$. The experimental measured absolute atomic hydrocarbon production of 0.51 ± 0.08 may be underestimated. In view of these discrepancies, further reinvestigation of the title reaction is still desirable.

6. Interstellar Implications

Because both $C(^3P)$ and propylene (C_3H_6) have been detected in the interstellar medium (ISM), the reaction between each other may have important implications. It is long known that reactions of zero or minute barriers are generally favored in the ISM. Then, the barrierless nature for the reaction of $C(^3P)$ with C_3H_6 makes the title reaction proceed very easily and lead to the major products $\mathbf{P_4}(^2CH_3CCCH_2 + {}^2H)$, $\mathbf{P_5}(^2CH_3CHCCH + {}^2H)$, and $\mathbf{P_7}(^2CH_2CCH + {}^2CH_3)$. The structure isomers CH_3CCCH_2 and CH_3CHCCH play important roles in pyrolysis of unsaturated hydrocarbons[31] and have received much attention.[32−38] The H atom is important in the H-containing system. The smallest conjugated hydrocarbon radical, C_3H_3, has received considerable attention because of its involvement in the ISM,[39−41] combustion flames,[42−44] and planetary atmosphere.[45] Up to now, a large number of studies have been reported on the C_3H_3 radical.[46−52] The CH_3 radical is also an important intermediate in the ISM driven by cosmic-ray ionization[53] as well as in the combustion process.[54] All of these aspects reinforce the importance of the title reaction in the ISM.

7. Reliability Assessment

We performed test calculations on the species **R** ($C(^3P) + C_3H_6$), $\mathbf{P_4}$ ($^2CH_3CCCH_2 + {}^2H$), $\mathbf{P_5}$ ($^2CH_3CHCCH + {}^2H$), $\mathbf{P_6}$ ($^1C_2H_2 + {}^3CH_3CH$), $\mathbf{P_7}$ ($^2CH_2CCH + {}^2CH_3$), **1**, **2a**, **2b**, **3**, **5a**, **TS1/2a**, **TS2a/2b**, **TS2a/3**, **TS2a/5a**, $\mathbf{TS2a/P_5}$, $\mathbf{TS2b/P_5}$, $\mathbf{TS2b/P_7}$, and $\mathbf{TS5a/P_6}$, which involved the most feasible pathways at the QCISD/6-311G(d,p) level, followed by the G3B3 single-point energy calculations. Surely, the high-level and more expensive method QCISD is expected to be superior to the B3LYP method. As shown in Figure 5, the structural parameters at both levels are generally in good agreement with each other. Most importantly, as shown in Table 3, the G3B3//B3LYP/6-311G(d,p) relative energies for these 18 species agree well with the corresponding G3B3//QCISD/6-311G(d,p) values with the largest deviation 0.9 kcal/mol of **TS1/2a**. Therefore, we expect that the G3B3//B3LYP/6-311G(d,p) method can provide reliable information for the $C(^3P) + C_3H_6$ reaction.

8. Conclusions

A detailed potential energy surface for the reaction of ground-state atomic carbon $C(^3P)$ with C_3H_6 was investigated at the B3LYP/6-311G(d,p) and G3B3 (single-point) levels. The main results can be summarized as follows: The $C(^3P)$ can barrierlessly attack the C=C double bond of C_3H_6 to form the three-membered ring isomer **1** CH_3-cCHCCH$_2$. Subsequently, **1** undergoes various isomerization and dissociation pathways leading to nine dissociation products. Among these nine products, $\mathbf{P_4}$ ($^2CH_3CCCH_2 + {}^2H$), $\mathbf{P_5}$ ($^2CH_3CHCCH + {}^2H$), and $\mathbf{P_7}$ ($^2CH_2CCH + {}^2CH_3$) should be the most feasible products and $\mathbf{P_6}$ ($^1C_2H_2 + {}^3CH_3CH$) should be the least feasible product. Other products, $\mathbf{P_1}(^2CH_3\text{-}cCHCCH + {}^2H)$, $\mathbf{P_2}(^2CH_3\text{-}cCCCH_2 + {}^2H)$, $\mathbf{P_3}(c^2CH_2CCH + {}^2CH_3)$, $\mathbf{P_8}(^1CCH_2 + {}^3CH_3CH)$, and $\mathbf{P_9}(^2HCC + {}^2C_2H_5)$ may have undetected yields. We expect that our results may be useful for deeply understanding the mechanism of the title reaction.

Acknowledgment. This work is supported by the National Natural Science Foundation of China (nos. 20773048).

References and Notes

(1) Clary, D. C.; Buonomo, E.; Sims, I. R.; Smith, I. W. M.; Geppert, W. D.; Naulin, C.; Costes, M.; Cartechini, L.; Casavecchia, P. *J. Phys. Chem. A* **2002**, *106*, 5541.
(2) Smith, I. W. M. *Chem. Soc. Rev.* **2003**, *31*, 137.
(3) Clary, D. C.; Haider, N.; Husain, D.; Kabir, M. *Astrophys. J.* **1994**, *422*, 416.
(4) Turner, B. E.; Herbst, E.; Terzieva, R. *Astrophys. J., Suppl. Ser.* **2000**, *126*, 427.
(5) Kaiser, R. I.; Le, T. N.; Nguyen, T. L.; Mebel, A. M.; Balucani, N.; Lee, Y. T.; Stahl, F.; Schleyer, P.v. R.; Schaefer, H. F., III *Faraday Discuss.* **2001**, *119*, 51.
(6) Casavecchia, P.; Balucani, N.; Cartechini, L.; Capozza, G.; Bergeat, A.; Volpi, G. G. *Faraday Discuss.* **2001**, *119*, 27.
(7) Kaiser, R. I.; Mebel, A. M. *Int. Rev. Phys. Chem* **2002**, *21*, 307.
(8) Haider, N.; Husain, D. *J. Chem. Soc., Faraday Trans.* **1993**, *89*, 7.
(9) Kaiser, R. I.; Lee, Y. T.; Suits, A. G. *J. Chem. Phys.* **1995**, *103*, 10395.
(10) Takayanagi, T. *J. Phys Chem. A* **2006**, *110*, 361.
(11) Mebel, A. M.; Kislov, V. V.; Hayasi, M. *J. Chem. Phys.* **2007**, *126*, 204310.
(12) Leonori, F.; Petrucci, R.; Segoloni, E.; Bergeat, A.; Hickson, K. M.; Balucani, N.; Casavecchia, P. *J. Phys Chem. A* **2008**, *112*, 1363.
(13) Kaiser, R. I.; Lee, Y. T.; Suits, A. G. *J. Chem. Phys.* **1996**, *105*, 8705.
(14) Kaiser, R. I.; Stranges, D.; Bevsek, H. M.; Lee, Y. T.; Suits, A. G. *J. Chem. Phys.* **1997**, *106*, 4945.
(15) Kaiser, R. I.; Stranges, D.; Lee, Y. T.; Suits, A. G. *Astrophys. J.* **1997**, *477*, 982.
(16) Chastaing, D.; James, P. L.; Sims, J. I.; Smith, I. W. M. *Phys. Chem. Chem. Phys* **1999**, *1*, 2247.
(17) Loison, J. C.; Bergeat, A. *Phys. Chem. Chem. Phys* **2004**, *6*, 5396.
(18) Li, Y.; Liu, H. L.; Huang, X. R.; Wang, D. Q.; Sun, C. C. *J. Phys. Chem. A* **2009**, *113*, 6800.
(19) Kaiser, R. I.; Mebel, A. M.; Chang, A. H. H.; Lin, S. H.; Lee, Y. T. *J. Chem. Phys.* **1999**, *110*, 10330.
(20) Schranz, H. W.; Smith, S. C.; Mebel, A. M.; Lin, S. H. *J. Chem. Phys.* **2002**, *117*, 7055.
(21) Mebel, A. M.; Kaiser, R. I.; Lee, Y. T. *J. Am. Chem. Soc.* **2000**, *122*, 1776.
(22) Kaiser, R. I.; Stranges, D.; Lee, Y. T.; Suits, A. G. *J. Chem. Phys.* **1996**, *105*, 8721.
(23) Sun, B. J.; Huang, C. Y.; Kuo, H. H.; Chen, K. T.; Sun, H. L.; Huang, C. H.; Tsai, M. F.; Kao, C. H.; Wang, Y. S.; Gao, L. G.; Kaiser, R. I.; Chang, A. H. H. *J. Chem. Phys.* **2008**, *128*, 244303.
(24) Hahndorf, I.; Lee, H. Y.; Mebel, A. M.; Lin, S. H.; Lee, Y. T.; Kaiser, R. I. *J. Chem. Phys.* **2000**, *113*, 9622.
(25) Balucani, N.; Lee, H. Y.; Mebel, A. M.; Kaiser, R. I. *J. Chem. Phys.* **2001**, *115*, 5107.
(26) Kaiser, R. I.; Sun, W.; Suits, A. G.; Lee, Y. T. *J. Chem. Phys.* **1997**, *107*, 8713.
(27) Nguyen, T. L.; Mebel, A. M.; Kaiser, R. I. *J. Phys. Chem. A* **2003**, *107*, 2990.
(28) Frisch, M. J.; Trucks, G. W.; Schlegel, H. B.; Scuseria, G. E.; Robb, M. A.; Cheeseman, J. R.; Zakrzewski, V. G.; Montgomery, J. A., Jr.; Stratmann, R. E.; Burant, J. C.; Dapprich, S.; Millam, J. M.; Daniels, A. D.; Kudin, K. N.; Strain, M. C.; Farkas, O.; Tomasi, J.; Barone, V.; Cossi, M.; Cammi, R.; Mennucci, B.; Pomelli, C.; Adamo, C.; Clifford, S.; Ochterski, J.; Petersson, G. A.; Ayala, P. Y.; Cui, Q.; Morokuma, K.; Malick, D. K.; Rabuck, A. D.; Raghavachari, K.; Foresman, J. B.; Cioslowski, J.; Ortiz, J. V.; Stefanov, B. B.; Liu, G.; Liashenko, A.; Piskorz, P.; Komaromi, I.; Gomperts, R.; Martin, R. L.; Fox, D. J.; Keith, T.; Al-Laham, M. A.; Peng, C. Y.; Nanayakkara, A.; Gonzalez, C.; Challacombe, M.; Gill, P. M. W.; Johnson, B. G.; Chen, W.; Wong, M. W.; Andres, J. L.; Head-Gordon, M.; Replogle, E. S.; Pople, J. A. *Gaussian 98*, revisionA.6; Gaussian, Inc.: Pittsburgh, PA, 1998.
(29) Curtiss, L. A.; Raghavachari, K.; Redfern, P. C.; Rassolov, V.; Pople, J. A. *J. Chem. Phys.* **1998**, *109*, 7764.
(30) Boboul, A. G.; Curtiss, L. A.; Redfern, P. C.; Raghavachari, K. *J. Chem. Phys.* **1999**, *110*, 7650.
(31) Nguyen, T. T.; King, K. D. *J. Phys. Chem.* **1981**, *85*, 3130.
(32) Marinov, N. M.; Pitz, W. J.; Westbrook, C. K.; Lutz, A. E.; Vincitore, A. M.; Senkan, S. M. In *27th Symposium (International) on Combustion Institute*; The Combustion Institute: Pittsburgh, PA, 1998; pp 605−613.
(33) Parker, C. L.; Cooksy, A. L. *J. Phys. Chem. A* **1999**, *103*, 2160.
(34) Marinov, N. M.; Pitz, W. J.; Westbrook, C. K.; Castaldi, M. J.; Senkan, S. M. *Combust. Soc. Technol.* **1996**, *117*, 211.
(35) Hansen, N.; Klippenstein, S. J.; Taatjes, C. A.; Miller, J. A.; Wang, J.; Cool, T. A.; Yang, B.; Yang, R.; Wei, L.; Huang, C.; Wang, J.; Qi, F.; Law, M. E.; Westmorelane, P. R. *J. Phys. Chem. A* **2006**, *110*, 3670.

(36) Hansen, N.; Miller, J. A.; Taatjes, C. A.; Wang, J.; Cool, T. A.; Law, M. E.; Westmoreland, P. R. *Proc. Combust. Inst.* **2007**, *31*, 1157.
(37) Yang, B.; Li, Y.; Wei, L.; Huang, C.; Wang, J.; Tian, Z.; Yang, R.; Sheng, L.; Zhang, Y.; Qi, F. *Proc. Combust. Inst.* **2007**, *31*, 555.
(38) Hansen, N.; Cool, T. A.; Westnoreland, P. R.; Kohse-Hõinghaus, K. *Prog. Energy Combust. Sci.* **2009**, *35*, 168.
(39) Herbst, E.; Leung, C. M. *Astrophys. J., Suppl. Ser.* **1989**, *69*, 271.
(40) Herbst, E. *Angew. Chem.* **1990**, *102*, 627.
(41) Küpper, J.; Merritt, J. M.; Miller, R. E. *J. Chem. Phys.* **2002**, *117*, 647.
(42) Kern, R. D.; Xie, K.; Chen, H. *Combust. Sci. Technol.* **1992**, *85*, 77.
(43) Rotzell, G. *J. Chem. Kinet.* **1985**, *17*, 637.
(44) Collin, G. J.; Deslauriers, G. R.; De Mare, G. R.; Poirier, R. A. *J. Phys. Chem.* **1990**, *94*, 134.
(45) Toublanc, D.; Parisot, J. P.; Brillet, J.; Gautier, D.; Raulin, F.; Mckay, C. P. *Icarus* **1995**, *113*, 2.
(46) Knyazev, V. D.; Slagle, I. R. *J. Phys. Chem. A.* **2002**, *106*, 5613.
(47) Lee, H.; Joo, S. K.; Kwon, L. K.; Choi, J. H. *J. Chem. Phys.* **2003**, *119*, 9337.
(48) Geppert, W. D.; Eskola, A. J.; Timonen, R. S.; Halonen, L. *J. Phys. Chem. A* **2004**, *108*, 4232.
(49) Lee, H.; Nam, M. J.; Choi, J. H. *J. Chem. Phys.* **2004**, *124*, 044311.
(50) Schüβler, T.; Roth, W.; Gerber, T.; Alcaraz, C.; Fischer, I. *Phys. Chem. Chem. Phys.* **2005**, *7*, 819.
(51) Wheeler, S. E.; Robertson, K. A.; Allen, W. D.; Schaefer, H. F., III *J. Phys. Chem. A* **2007**, *111*, 3819.
(52) Georgievskii, Y.; Miller, J. A.; Klippenstein, S. J. *Phys. Chem. Chem. Phys.* **2007**, *9*, 4259.
(53) Herbst, E.; Klemperer, W. *Appl. Phys. Lett.* **1973**, *185*, 505.
(54) Hughes, K. J.; Turanyi, T.; Clague, A. R.; Pilling, M. J. *Int. J. Chem. Kinet.* **2001**, *33*, 513.

JP903844P